

# Abcb4-defect cholangitis mouse model with hydrophobic bile acid composition by *in vivo* liver-specific gene deletion

Kota Tsuruya<sup>1,2,\*</sup>, Keiko Yokoyama<sup>2,3,\*</sup>, Yusuke Mishima<sup>1,2</sup>, Kinuyo Ida<sup>2</sup>, Takuma Araki<sup>2,3</sup>, Satsuki Ieda<sup>1</sup>, Masato Ohtsuka<sup>2</sup>, Yutaka Inagaki<sup>4</sup>, Akira Honda<sup>5,6</sup>, Tatehiro Kagawa<sup>1,\*</sup>, and Akihide Kamiya<sup>2,\*</sup>

<sup>1</sup>Division of Gastroenterology, Department of Internal Medicine, <sup>2</sup>Department of Molecular Life Sciences, <sup>3</sup>Support Center of Medical Research and Education, and <sup>4</sup>Center for Matrix Biology and Medicine, Tokai University School of Medicine, Isehara, Kanagawa, Japan; <sup>5</sup>Joint Research Center, and <sup>6</sup>Department of Gastroenterology and Hepatology, Tokyo Medical University Ibaraki Medical Center, Ibaraki, Japan

**Abstract** Progressive familial intrahepatic cholestasis (PFIC) is a liver disease that occurs during childhood and requires liver transplantation. ABCB4 is localized along the canalicular membranes of hepatocytes, transports phosphatidylcholine into bile, and its mutation causes PFIC3. Abcb4 gene-deficient mice established as animal models of PFIC3 exhibit cholestasis-induced liver injury. However, their phenotypes are often milder than those of human PFIC3, partly because of the existence of large amounts of less toxic hydrophilic bile acids synthesized by the rodent-specific enzymes Cyp2c70 and Cyp2a12. Mice with double deletions of Cyp2c70/Cyp2a12 (CYPDKO mice) have a human-like hydrophobic bile acid composition. PFIC-related gene mutations were induced in CYPDKO mice to determine whether these triple-gene-deficient mice are a better model for PFIC. To establish a PFIC3 mouse model using CYPDKO mice, we induced abcb4 gene deletion *in vivo* using adeno-associated viruses expressing SaCas9 under the control of a liver-specific promoter and abcb4-target gRNAs. Compared to Abcb4-deficient wild-type mice, Abcb4-deficient CYPDKO mice showed more pronounced liver injury along with an elevation of inflammatory and fibrotic markers. The proliferation of intrahepatic bile ductal cells and hematopoietic cell infiltration were also observed. CYPDKO/abcb4-deficient mice show a predominance of taurine-conjugated chenodeoxycholic acid and lithocholic acid in the liver. In addition, phospholipid levels in the gallbladder bile were barely detectable. Mice with both human-like bile acid composition and Abcb4-defect exhibit severe cholestatic liver injury and are useful for studying human cholestatic diseases and developing new treatments.

**Supplementary key words** progressive familial intrahepatic cholestasis • genome editing • bile acid composition • adeno-associated virus

The bile is composed of water, bile acids, bilirubin, cholesterol, and fatty acids. Bile acids, the major components of bile, activate various signaling pathways by binding to specific nuclear receptors, such as the farnesoid X receptor (FXR) (1, 2). The disruption of the bile acid transport pathway in hepatocytes causes liver damage and inflammation, leading to liver fibrosis, cirrhosis, and hepatocellular carcinoma. Many hepatocyte transporters are involved in the influx and outflow of intracellular bile, and mutations or defects in these transporters and related genes can cause cholestasis and cholangitis including progressive familial intrahepatic cholestasis (PFIC) (3). In humans, PFIC occurs during childhood and requires a liver transplant. To date, at least six PFIC-related genes have been identified: *ATP8B1*, *ABCB11*, *ABCB4*, *TJP2*, *NR1H4*, and *MYO5B* (4). *ABCB4*, which belongs to the ATP-binding cassette transporter family, is located along the canalculus of hepatocytes (5) and transports phosphatidylcholine into bile (6, 7). The bile fluid contains phospholipids and cholesterol, which play a role in decreasing the toxic detergent effects of bile. Therefore, *ABCB4* deficiency results in cholangitis and cholestasis-induced liver injury. Mice lacking PFIC-related genes have been used to reproduce the symptoms of human PFIC in an experimental model (8, 9). *Abcb4*-deficient mice lack bile phospholipids and exhibit liver injury owing to increased bile toxicity. AST and ALT levels are elevated at 4–8 weeks of age and cirrhosis with fibrosis develops at 8–12 weeks. *Abcb4* suppression also induces hepatocellular carcinoma formation in older mice (10). However, the symptoms in these mouse models are generally milder than those in human PFIC3, which progresses rapidly and severely and requires liver transplantation. This phenotypic difference may be

\*These authors have contributed equally to this work.

\*For correspondence: Akihide Kamiya, [kamiyaa@tokai.ac.jp](mailto:kamiyaa@tokai.ac.jp); Tatehiro Kagawa, [kagawa@tokai.ac.jp](mailto:kagawa@tokai.ac.jp).

attributable to the differences in bile acid composition between humans and mice (11). Most bile acids in mice are hydrophilic muricholic acids (MCAs) because mice express specific bile acid-metabolizing enzymes that are not found in humans: Cyp2c70 and Cyp2a12 (12). Mice, but not humans, have a metabolic pathway that converts hydrophobic bile acids to hydrophilic MCAs and cholic acid (CA) using Cyp2c70/Cyp2a12. Unlike wild-type mice, Cyp2c70/Cyp2a12 double-deficient mice (CYPDKO) lack MCA and have a bile acid composition similar to that of humans, containing more hydrophobic bile acids. We considered utilizing CYPDKO mice to reproduce human PFIC because these mice with human-like bile acids would manifest more severe liver injury than wild-type mice.

The liver maintains homeostasis and participates in the metabolism of drugs, lipids, cholesterol, and bile acids. Gene transgenic and knockout mice are useful for functional analyses of transcription-related factors, metabolic enzymes, and transporters that regulate these metabolic pathways. Genome-editing enzymes such as CRISPR/Cas9 are useful for the rapid establishment of gene knock-out and knock-in mice (13–15). An *in vivo* genome editing method using Cas9 transgenic mice has been reported (16). However, multiple steps and genetically modified mice are required to generate tissue-specific, genetically deficient mice. The introduction of the Cas9 protein using an adeno-associated virus (AAV) has been recently reported to enable direct genome editing in adults (17, 18). AAV allows easy *in vivo* gene transfer to various organs such as the liver (19, 20). For example, gene deletion and suppression mouse models have been established using Cas9-induced indel gene editing and the Cas9KRAB fusion protein in the liver (21). Studies on *in vivo* genome editing and gene therapy for liver diseases, such as hemophilia, have reported the use of an AAV-dependent Cas9 delivery system (22–24), suggesting that these AAV-dependent genome-editing systems are useful for liver-specific gene knockout methods in normal mice without the Cas9 transgene in the genome (25).

In this study, we generated PFIC model mice with a human bile acid-like hydrophobic composition and analyzed the species differences in bile acid composition in cholestasis models. The induction of a new gene mutation in CYPDKO mice requires extensive genetic engineering and mating. Therefore, we used a system that somatically induces gene deletion using AAV. Liver-specific gene-deficient mice were established within a short period by expressing SaCas9 under the control of a human antitrypsin (hAAT) promoter. We induced Abcb4-deficiency in CYPDKO and wild-type C57BL/6J (B6) mice to compare PFIC physiology with different hydrophobic and hydrophilic bile acid compositions. Abcb4 depletion in CYPDKO mice induced more severe liver damage and fibrosis within a shorter period than in wild-type mice. This is the first study to

demonstrate the importance of species-specific differences in bile acid composition in an animal model of cholestasis. This PFIC mouse model is a useful tool for studying human PFIC and developing new treatments.

## MATERIALS AND METHODS

### Experimental animals

C57BL6/J mice were purchased from Nihon SLC and CLEA Japan, Inc. Mutant green fluorescent protein (GFP) transgenic mice (#197) have also been established (26). Cyp2a12/2c70 double knockout (CYPDKO) mice have been described previously (12). Mice were maintained on a 12-h dark/light cycle with free access to food (CA-1) and water. Ursodeoxycholic acid (UDCA) water (2 mM), prepared by diluting UDCA (DS Pharma Animal Health Co), was administered as drinking water to CYPDKO mice and changed to normal water 1 week before AAV injection. In CYPDKO mice, the increased hydrophobicity of bile acids caused a decrease in reproductive ability, and 20%–25% of mice died after weaning. Feeding UDCA to CYPDKO mice not only ameliorated frequent miscarriages and unexpected deaths after weaning but also suppressed spontaneous liver injury (27). In addition, the discontinuation of UDCA returned the BA composition to the original human-like composition within two weeks (27). Since samples were collected 4–5 weeks after AAV administration, total 5–6 weeks had passed since UDCA administration was stopped. These mice were sacrificed between 12:00 and 16:00 under anesthesia with isoflurane after fasting for 4 h with free access to water. In these Abcb4-deficient studies, male CYPDKO and C57BL6/J mice (10–13 weeks old) were used for AAV injection because of spontaneous liver injury in female CYPDKO mice. The animal experimental protocols were approved by the Institutional Animal Care and Use Committee of Tokai University (approval numbers: 243,010, 232,006, 232,008, 221,011, 221,105, 211,068, 201,051, and 204,009).

### Virus construction

A liver-specific promoter-loaded version of the rAAV2-LSP1 vector (20) and the rAAV2 vector was used to introduce SaCas9 (Takara Bio Inc.). A rAAV2 vector containing the human-U6 promoter was used for gRNA expression. The gRNA sequences were designed using CRISPOR (<http://crispor.tefor.net/>). The target sequences of the gRNA are listed in supplemental Table S1. AAV was produced by co-transfecting HEK293T cells with the AAV8 capsid (Penn Vector Core, University of Pennsylvania) and helper plasmids (Takara Bio Inc.). HEK293T cells were cultured in Dulbecco's modified Eagle's medium (DMEM) supplemented with 10% fetal bovine serum and 1% penicillin-streptomycin-L-glutamine. After 16 h, the medium was replaced with DMEM supplemented with 2% fetal bovine serum and 1% penicillin-streptomycin-L-glutamine solution and cultured for 2 days, and all cells were collected. AAV was purified from the cells and concentrated using the AAVPro Purification Kit (Takara Bio Inc.). AAV titers were measured using the AAVpro Titration Kit Ver2 (Takara Bio, Inc.) for RT-PCR.

### AAV injection into mice for gene deletion

After anesthesia was induced through isoflurane inhalation via the oral cavity, AAVs expressing SaCas9 in

combination with either EGFP-gRNA or three types of gRNAs for target genes were administered intraperitoneally ( $2.0\text{--}3.0 \times 10^{11}$  vg/mouse). For *Abcb4* deletion, 10–13-week-old CYPDKO and C57BL/6J male mice were used. Mice infected with AAVs expressing SaCas9 and EGFP-gRNA, or mice without AAVs were used as negative controls (NTC). To select mice for AAV injection of either EGFP control gRNA or target gene gRNAs, mice of approximately the same weight were randomly selected. One CYPDKO/*Abcb4*-deficient mouse was excluded from the analyses because of liver atrophy caused by unknown reasons.

### Statistical analysis

Student's *t*-tests and one way ANOVA (for analysis of more than three groups) were performed using Prism7 (GraphPad Software), SDs were calculated, and statistically significant differences were determined.

All other methods are shown in the [Supporting Materials](#) and [supplemental Tables S1 and S2](#).

## RESULTS

### Liver-specific genome-editing using AAV and CRISPR/Cas9

A system for identifying genome editing efficiency by introducing gRNA around the mutation site in mutant GFP transgenic mice has been reported (26), in which Cas9 and gRNA introduction causes an indel mutation that corrects the reading frame of the gene with a certain probability and restores mutant-GFP activity. Therefore, we used this system to analyze the liver-specific promoter activity during AAV infection ([supplemental Fig. S1A](#)). A liver-specific AAV vector reportedly consists of an Apolipoprotein E enhancer, a hAAT promoter, and a WPRE sequence involved in RNA stabilization (20). Three SaCas9 expression vectors, with or without these components, were constructed, and the activity of each vector was evaluated ([supplemental Fig. S1B](#)). Mutant GFP-mice (9-week-old) were infected with AAV-a, b, and c vectors and AAV expressing gRNA against mutant GFP ( $1.1 \times 10^{11}$  vg/mouse), and livers were analyzed with a fluorescence microscope after 4 weeks of infection. When mutant-GFP adult mice were infected with these liver-specific SaCas9-expressing AAVs and human U6 promoter gRNA-expressing AAVs, a similar recovery of GFP fluorescence was observed for all three expression vectors, suggesting that the hAAT promoter was sufficient for hepatic Cas9 expression ([supplemental Fig. S1C](#)). We also analyzed whether genome editing by the hAAT-promoter AAV was possible in juvenile mice. Mutant GFP-mice (2-week-old) were transfected with AAV-c and AAV expressing gRNA against mutant GFP ( $0.7\text{--}1.2 \times 10^{11}$  vg/mouse), and livers and other organs were analyzed with a fluorescence microscope after 2–8 weeks. Significant GFP fluorescence was observed in the liver, whereas no recovery of luminescence was observed in other organs ([supplemental Fig. S1D, E](#)). Therefore, we found that a short hAAT

promoter expressing SaCas9 AAV is sufficient as an expression control region to enable liver-specific genome editing.

### Effect of *Abcb4* deficiency on human and mouse bile acid composition

As shown earlier, the combination of the hAAT promoter and SaCas9 efficiently induced liver-specific gene deletions. Therefore, using AAV, we introduced SaCas9 and *Abcb4*-gRNA into CYPDKO mice, which are human bile acid-like model mice, and wild-type C57BL/6J mice (control) to induce *Abcb4* deletion ([Fig. 1A, B](#)). Co-introduction of the liver-specific promoter SaCas9 and the three gRNAs for *Abcb4* using AAVs efficiently induced target gene deletion. We compared the relationship between changes in bile acid composition and *Abcb4*-deficiency in both male wild-type and CYPDKO mice. Almost 4–5 weeks after the introduction of AAV, the liver, other tissues, and serum were collected and analyzed. *Abcb4* deficiency did not affect body weight. The liver/body weight ratio increased in both CYPDKO and wild-type mice with *Abcb4* deletion ([Fig. 1C](#)). Similar to previous results (28), serum levels of liver injury markers (AST, ALT, and ALP) also tended to be elevated following *Abcb4* deletion in the wild-type mice, whereas the upregulation of injury markers in WT/*Abcb4*-deficient mice was slight because of short-term gene deletion (4–5 weeks after AAV injection) compared to previous gene deletion studies. In contrast, liver injury markers were significantly increased in CYPDKO/*Abcb4*-deficient mice, indicating that more severe liver injury was induced by the combination of *Abcb4* deletion and human-like bile acid composition, even within a short period ([Fig. 1D](#)). In addition, a slight increase in total cholesterol and triglyceride serum levels was observed in the CYPDKO/*Abcb4*-deficient mice ([Fig. 1E](#)).

Next, total bile acid and bilirubin serum levels were measured. Both *Abcb4*-deficient mice were found to have elevated total bile acid serum levels, indicating that *Abcb4* deletion induced cholestasis within a short period in both CYPDKO and wild-type mice ([Fig. 2A](#)). In contrast, serum total bilirubin (Bil) levels did not increase ([Fig. 2B](#)).

Bile is composed mainly of bile acids, cholesterol, and phospholipids. Quantitative analysis of these components showed that the amount of total bile acids in the gallbladder bile was higher in CYPDKO mice than in wild-type mice ([Fig. 2C](#)). Furthermore, in *Abcb4* gRNA-treated mice, almost no phospholipids were detected in the bile, indicating that *Abcb4*-genome editing hepatocytes had defective phospholipid transporters. Furthermore, cholesterol levels were reduced owing to *Abcb4* deficiency. These results indicate that the bile of CYPDKO/*Abcb4*-deficient mice had reduced cholesterol and phospholipid levels and a high bile acid composition. Thus, the expression of bile and

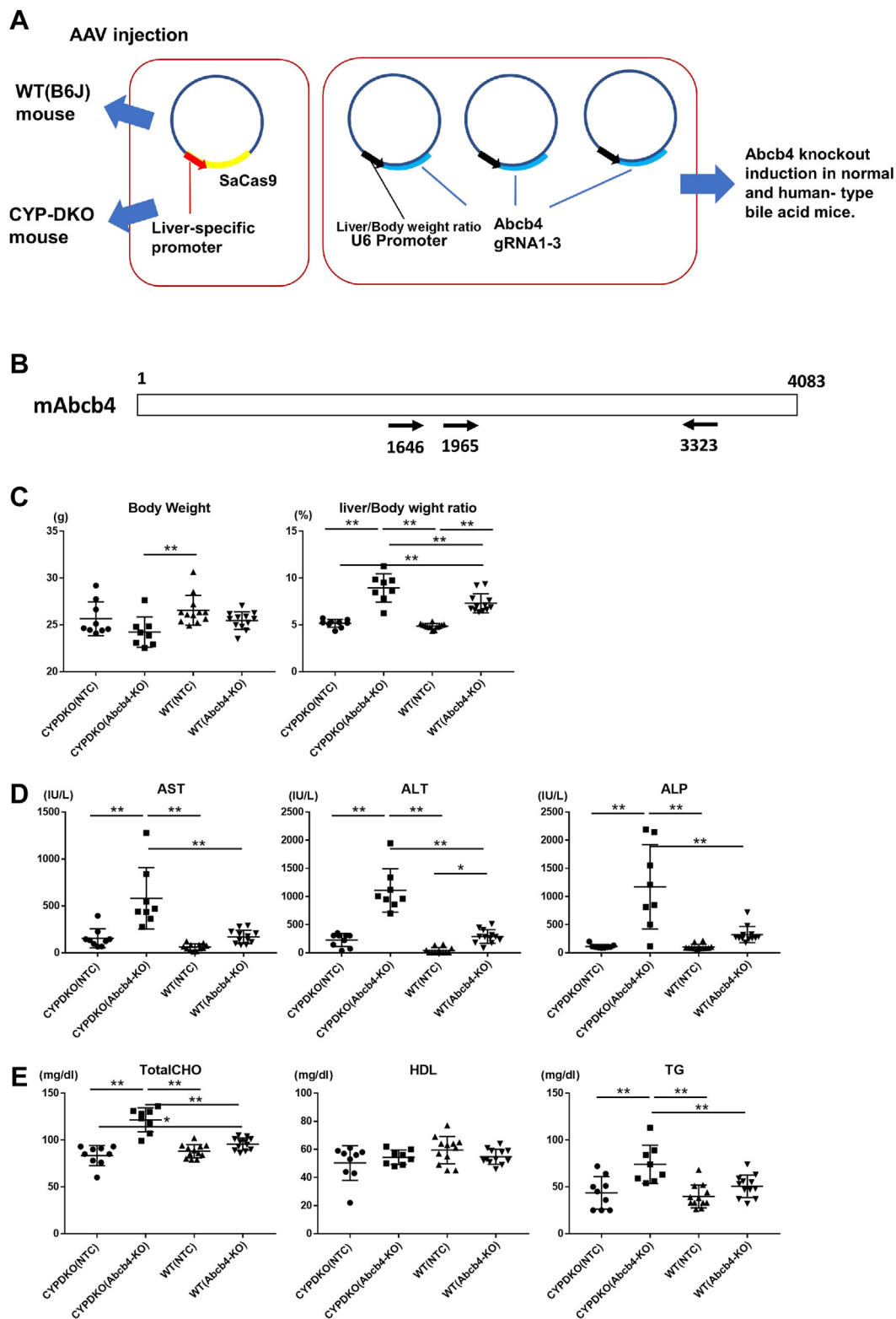


**Fig. 1.** Effect of *Abcb4* deficiency in human bile acid-model by AAV-triple CRISPR method. A: Generation of liver-specific *Abcb4*-deletion mice by the triple CRISPR method. B: Three gRNAs against the *Abcb4* gene. AAVs expressing gRNAs targeting the indicated sites in the CDS region were generated. C: Changes in body weight and liver/body weight ratio. D: Changes in liver-injury markers serum levels. E: Changes in serum total cholesterol (TotalChol), HDL, and triglycerides (TG). (n = 9 for CYPDKO/NTC, n = 8 for CYPDKO/*Abcb4*-KO, n = 12 for WT/NTC, and n = 12 for WT/*Abcb4*-KO). Results are represented as mean  $\pm$  SD (one-way ANOVA, \* $P$  < 0.05, \*\* $P$  < 0.01).



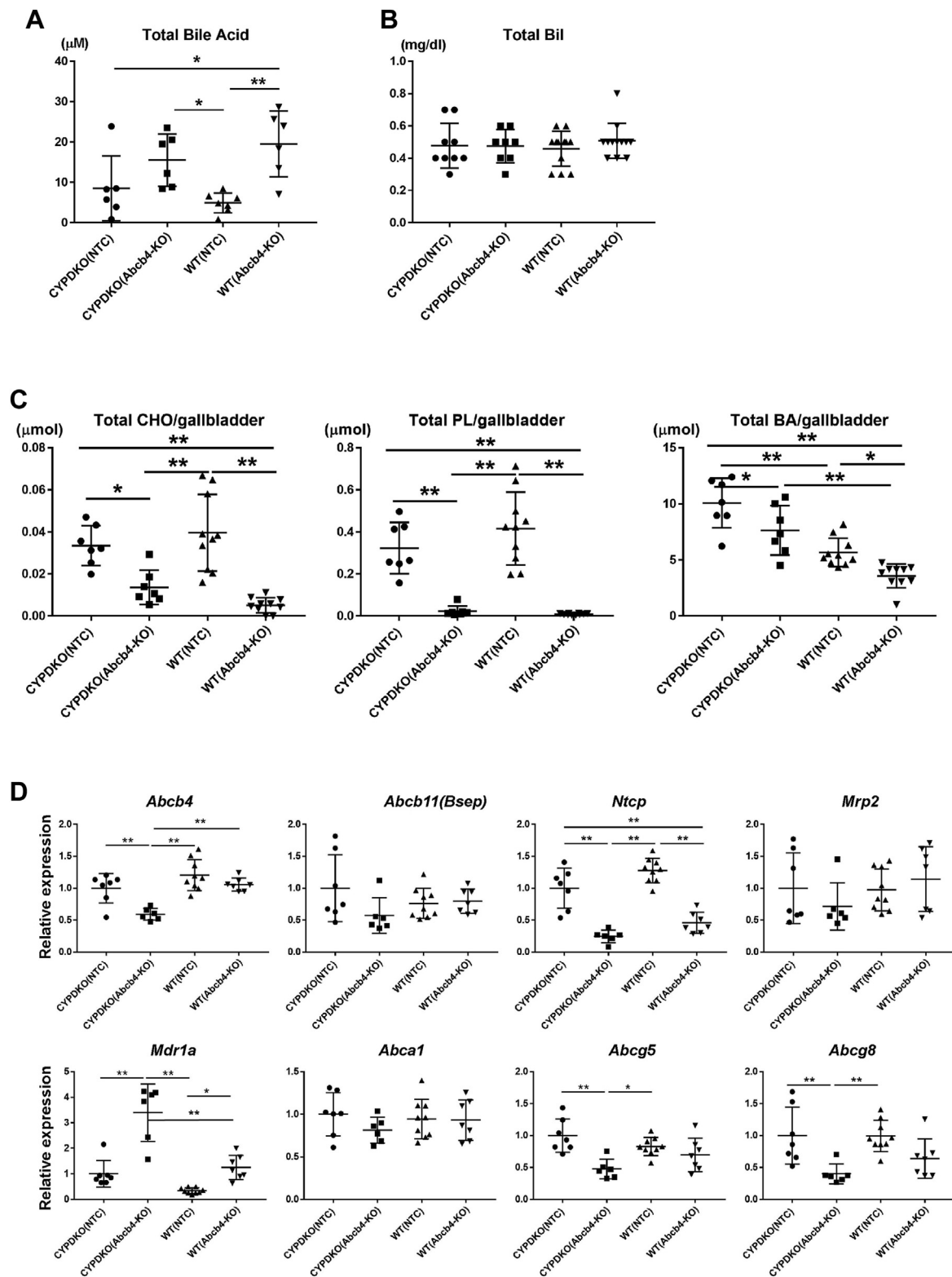


**Fig. 2.** Bile acid and cholesterol levels in the serum and gallbladder derived from CYPDKO/Abcb4-deficient mice. A: changes in serum total bile acid levels (n = 6 for CYPDKO/NTC, n = 6 for CYPDKO/Abcb4-KO, n = 7 for WT/NTC, and n = 6 for WT/Abcb4-KO). B: Changes in serum total bilirubin (Bil) levels (n = 9 for CYPDKO/NTC, n = 8 for CYPDKO/Abcb4-KO, n = 12 for WT/NTC, and n = 12 for WT/Abcb4-KO). C: Changes in cholesterol (CHO), phospholipid (PL), and total bile acid (BA) levels derived from the gallbladder bile (n = 7 for CYPDKO/NTC, n = 7 for CYPDKO/Abcb4-KO, n = 10 for WT/NTC, and n = 10 for WT/Abcb4-KO). D: Gene expression changes of bile acid and cholesterol metabolism-related genes in the liver. The expression of genes in CYPDKO/NTC mouse livers was set to 1.0 (n = 7 for CYPDKO/NTC, n = 6 for CYPDKO/Abcb4-KO, n = 9 for WT/NTC, and n = 7 for WT/Abcb4-KO). Results are represented as mean  $\pm$  SD (one-way ANOVA, \* $P$  < 0.05, \*\* $P$  < 0.01).

cholesterol transporters in hepatocytes was analyzed (Fig. 2D). There was almost no change in *Abcb4* mRNA expression in *Abcb4*-deficient wild-type mice. In contrast, the amount of mRNA was almost halved down-regulated in *Abcb4*-deficient CYPDKO-mice. Since a certain level of mRNA expression was observed in both *Abcb4*-deficient mice, it was suggested that mutant or shortened *Abcb4* mRNAs existed in this genome editing model despite the functional loss of *Abcb4* such as the absence of phospholipids in the gallbladder bile (Fig. 2C, D). In addition, changes in the expression of *Abcb11*, *Mrp2*, and *Abcal* were barely observed following *Abcb4* deletion. The expression of *Ntcp*, which is involved in the uptake of bile acids from the small intestine into hepatocytes, was decreased by *Abcb4* deficiency, indicating changes in the bile enterohepatic circulatory system. Furthermore, the expression of *Abcg5* and *Abcg8*, which are involved in cholesterol excretion from hepatocytes to bile, was decreased by *Abcb4* deficiency in CYP/DKO mice, consistent with the decrease in cholesterol levels in the gallbladder bile. In contrast, *Mdr1a* expression increased in CYPDKO/*Abcb4*-deficient mice, which may be a response to severe liver injury.

#### ***Abcb4* deficiency with hydrophobic bile acid composition induced liver inflammation, bile duct hyperplasia, and fibrosis**

We analyzed bile ductal cell proliferation and hematopoietic cell infusion induced by *Abcb4* deletion. In a normal genetic background, *Abcb4* deletion non-significantly increased the proliferation of K19-positive bile ductal cells around the portal veins (Fig. 3A, B, WT/*Abcb4*-KO). Human-like bile acid composition in CYPDKO mice (CYPDKO/NTC) alone does not cause bile duct hyperplasia. In contrast, the combination of *Abcb4* deletion and human-like bile acid composition (CYPDKO/*Abcb4*-KO) resulted in periportal CD45-positive hematopoietic cell infiltration, consistent with the exacerbation of liver injury as shown by serum marker levels, leading to significantly increased K19-positive bile ductal cell proliferation (Fig. 3B, right panels).

We analyzed changes in gene expression in the liver following *Abcb4* deletion. The expression of inflammatory cytokines (TNF- $\alpha$  and IL-1 $\beta$ ) and fibrosis-related TGF- $\beta$  was increased when *Abcb4*-gene deletion was induced in both CYPDKO and wild-type mice (Fig. 4A). Collagen 1 $\alpha$ 1 and TIMP1 were significantly upregulated in CYP/DKO/*Abcb4*-deficient mice, suggesting the importance of hydrophobic bile acid composition in liver fibrosis. In addition, smooth muscle actin ( $\alpha$ SMA), an activated stellate cell marker, was induced by *Abcb4* deletion. Next, liver fibrosis caused by collagen fiber deposition was analyzed because the expression of liver fibrosis marker genes was upregulated by *Abcb4*-deletion in CYPDKO mice. As shown in the

quantitative results, a slight deposition of collagen fibers was observed around the periportal bile duct structure in mice with *Abcb4* deficiency alone. In CYPDKO/*Abcb4* mice, strong fibrosis was observed around the hyperplastic bile ducts within a relatively short period (almost 4–5 weeks) of *Abcb4* deficiency (Fig. 4B). Thus, *Abcb4* deficiency in a human bile acid-like composition may induce stronger liver injury and fibrosis than that in mice with a hydrophilic bile acid composition.

#### **Changes in intrahepatic bile acid and lipid composition caused by *Abcb4* deficiency**

*Abcb4* deficiency alters bile acid composition in the liver. We analyzed whether the bile acid composition in the whole liver was altered by *Abcb4* deletion in wild-type and CYPDKO mice using Liquid Chromatography-Mass Spectrometry (Fig. 5A and supplemental Table S3). In wild-type mice, most bile acids are taurine-conjugated, as previously reported (12), and taurine-conjugated MCAs are abundant. *Abcb4* deficiency resulted in increased levels of taurine-conjugated CA and MCA in the wild-type genetic background. In contrast, free and taurine-conjugated MCAs were hardly detected in the livers of CYPDKO mice, whereas other taurine-conjugated bile acids such as chenodeoxycholic acid (TCDCA), deoxycholic acid (TDCA), lithocholic acid (TLCA), and TUDCA were elevated. In the CYPDKO genetic background, free and taurine-conjugated CDCA and LCA levels were increased following *Abcb4* deletion. The ratio of bile acid composition revealed that wild-type mice mainly had MCA, TCA, and TMCA in the liver (supplemental Fig. S2). In contrast, CYPDKO mice had few MCA and TMCA. CYPDKO/NTC mice mainly had TDCA (almost 40%), whereas CYPDKO/*Abcb4* mice mainly had TCDCA (almost 45%).

Total bile acid levels in the whole liver remained unchanged in CYPDKO/NTC mice. In contrast, total liver bile acid levels were significantly increased by *Abcb4* deletion in both wild-type and CYPDKO mice, suggesting that liver cholestasis occurred due to *Abcb4* deletion (Fig. 5B). We then calculated the hydrophobicity index (HI) of the bile acid composition in the liver. Wild-type mice, which contain more hydrophilic bile acids such as MCA, showed a low HI regardless of the presence or absence of *Abcb4*. In contrast, CYPDKO mice, which lacked the MCA, showed a high HI (Fig. 5C). Therefore, it is thought that the degree of liver damage is suppressed, even in WT/*Abcb4*-deficient mice, which have a high amount of intrahepatic bile acids.

Bile acid synthesis is regulated by several CYP family genes. Analysis of bile acid synthase gene expression in the liver revealed that *Cyp7b1* and *Cyp27a1* were downregulated by *Abcb4* deletion in both wild-type and CYPDKO mice (Fig. 6A). CYPDKO-induced

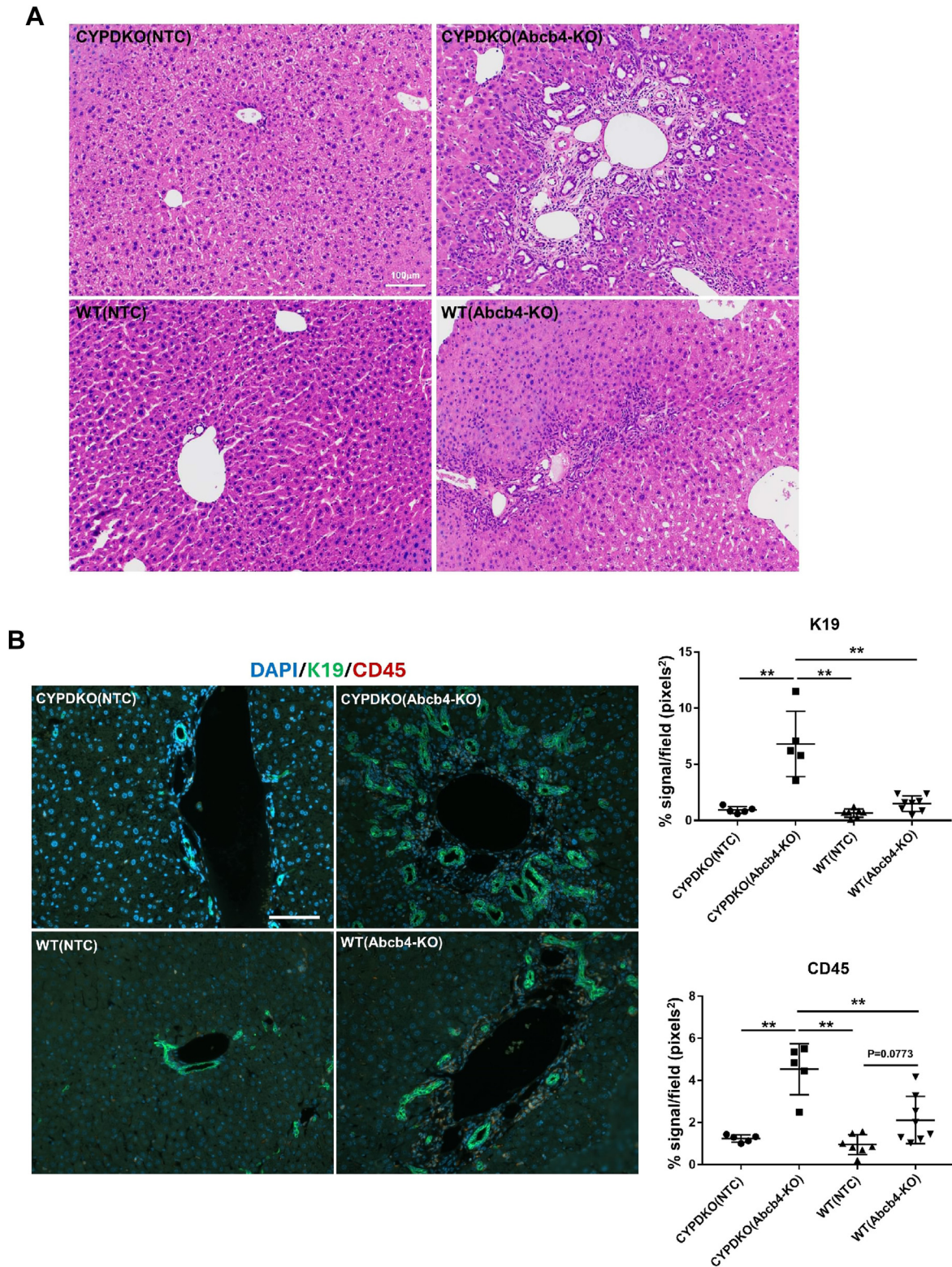


**Fig. 3.** Morphological changes in CYPDKO/Abcb4-deficient mouse liver. A and B: induction of blood infiltration and bile duct hyperplasia by Abcb4 deficiency. Hematoxylin and Eosin staining (A) and K19 and CD45 immunostaining (B) were performed. B (right panels): K19 and CD45 stains quantified the amount of biliary cell proliferation and hematopoietic cell infusion using the ImageJ software (n = 5 for CYPDKO/NTC mouse livers, n = 5 for CYPDKO/Abcb4-KO mouse livers, n = 7 for WT/NTC mouse livers, and n = 8 for WT/Abcb4-KO mouse livers). White line, 100  $\mu$ m. Results are represented as mean  $\pm$  SD (one-way ANOVA, \* $P$  < 0.05, \*\* $P$  < 0.01).



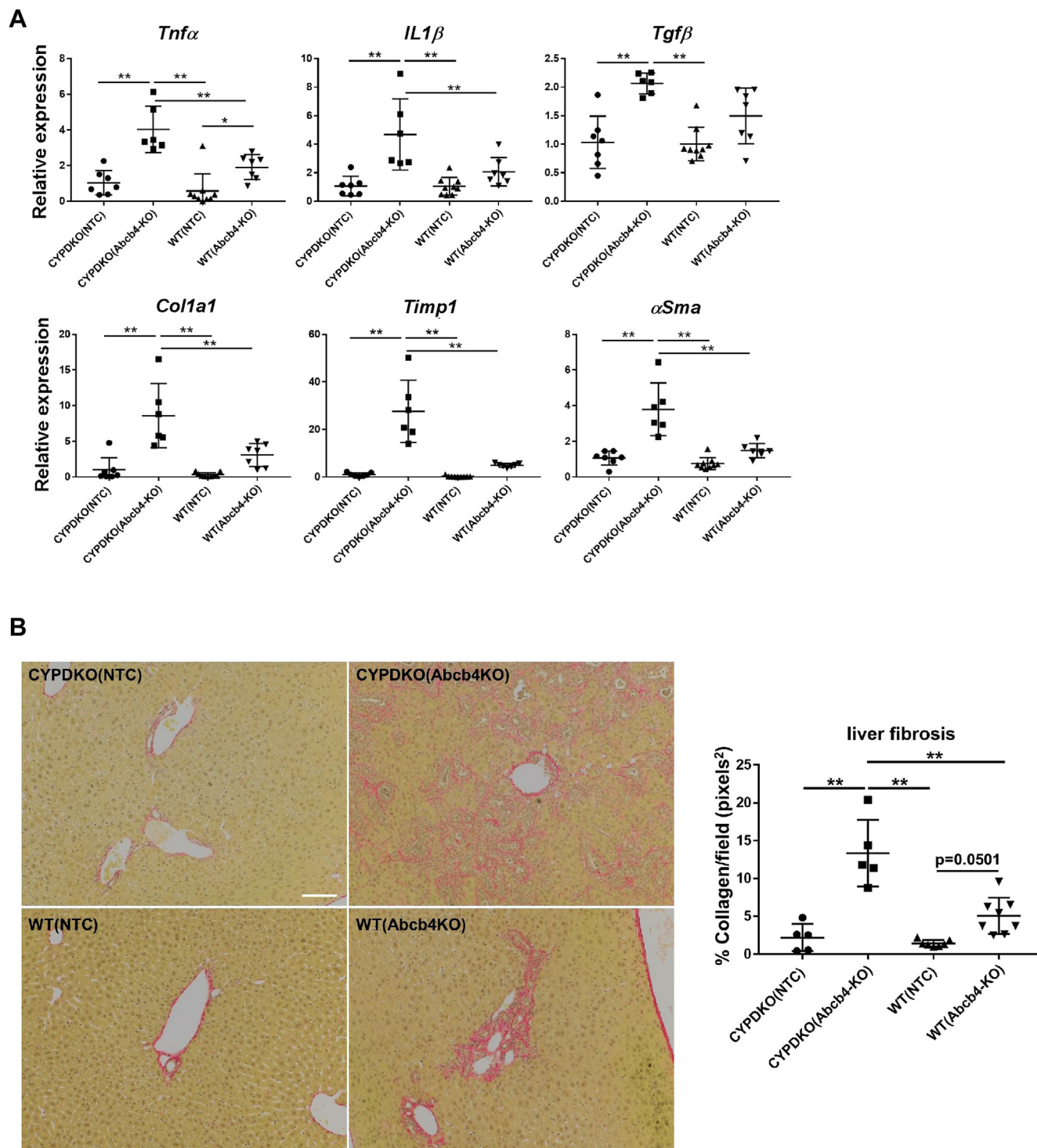


**Fig. 4.** Inflammatory and fibrosis in CYPDKO/Abcb4-deficient mice. A: gene expression changes of inflammatory and fibrotic markers in the liver. The expression of genes in CYPDKO/NTC mouse livers was set to 1.0 ( $n = 7$  for CYPDKO/NTC,  $n = 6$  for CYPDKO/Abcb4-KO,  $n = 9$  for WT/NTC, and  $n = 7$  for WT/Abcb4-KO). (B) Analysis of intrahepatic fibrosis with Sirius red staining. B (right panel): Sirius red stain was performed to visualize the liver fibers and quantify the amount of liver fibers using the ImageJ software ( $n = 5$  for CYPDKO/NTC mouse livers,  $n = 5$  for CYPDKO/Abcb4-KO mouse livers,  $n = 7$  for WT/NTC mouse livers, and  $n = 8$  for WT/Abcb4-KO mouse livers). White line, 100  $\mu$ m. Results are represented as mean  $\pm$  SD (one-way ANOVA, \* $P$  < 0.05, \*\* $P$  < 0.01).

human bile acid-like changes decrease Cyp8b1 expression. In particular, Cyp8b1 expression was barely detectable in CYPDKO/Abcb4-deficient mice. Abcb4-

deletion does not significantly suppress Cyp7a1 expression in wild-type or CYPDKO mice. Expression of Nr1h4 (Fxr) was downregulated by Abcb4 deletion



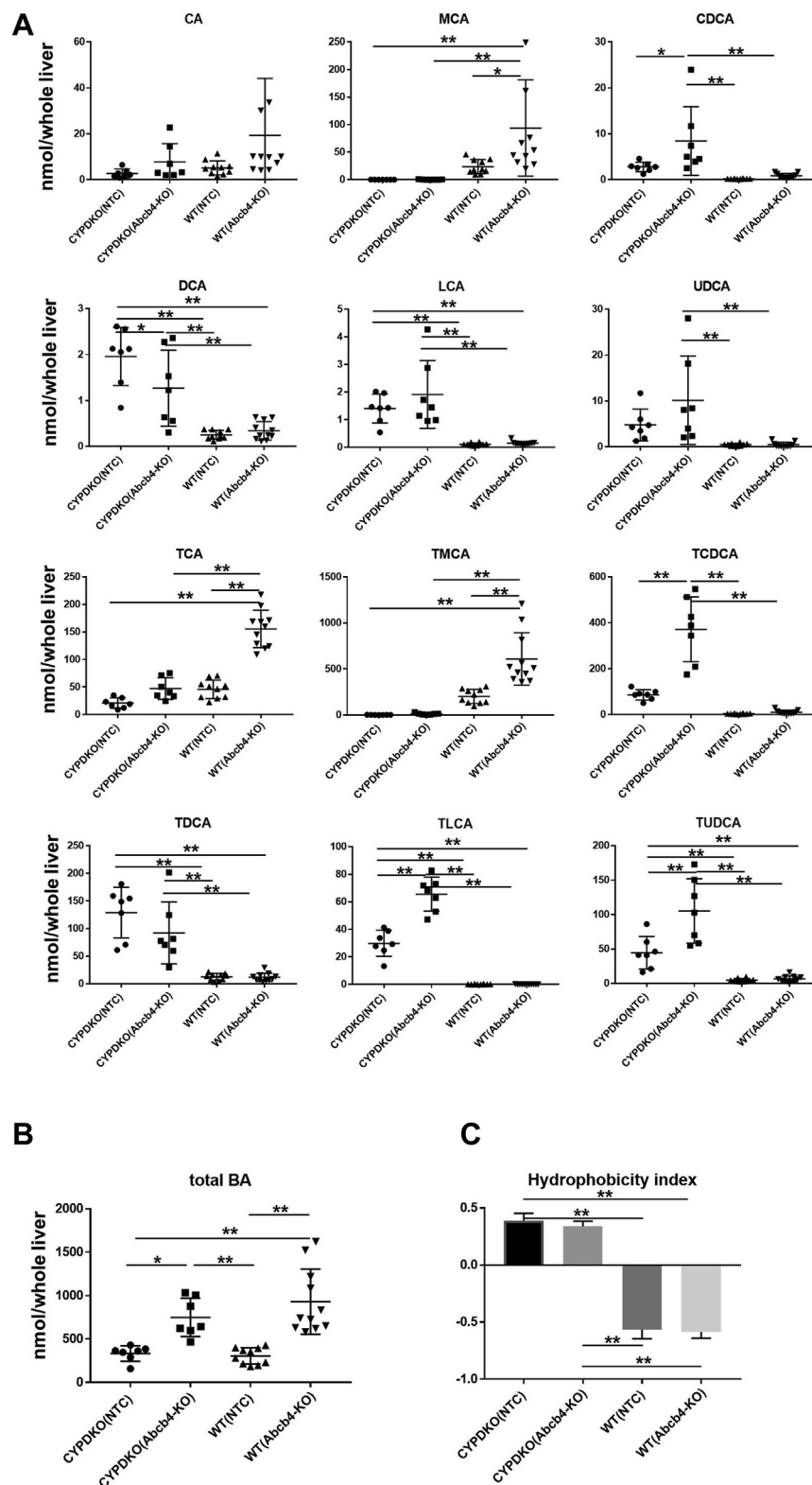


**Fig. 5.** Bile acid composition in the liver of CYPDKO/Abcb4-deficient mice. A and B: Level changes of various and total bile acids in the whole liver derived from WT and CYPDKO mice with Abcb4 deficiency. C: the hydrophobicity indices of total bile acid in the liver. Hydrophobicity index was calculated as a percentage-weighted mean of individual bile acid hydrophobicity as shown in [supplemental Table S3](#) (n = 7 for CYPDKO/NTC mouse livers, n = 7 for CYPDKO/Abcb4-KO mouse livers, n = 10 for WT/NTC mouse livers, and n = 11 for WT/Abcb4-KO mouse livers). Results are represented as mean  $\pm$  SD (one-way ANOVA, \* $P$  < 0.05, \*\* $P$  < 0.01.).

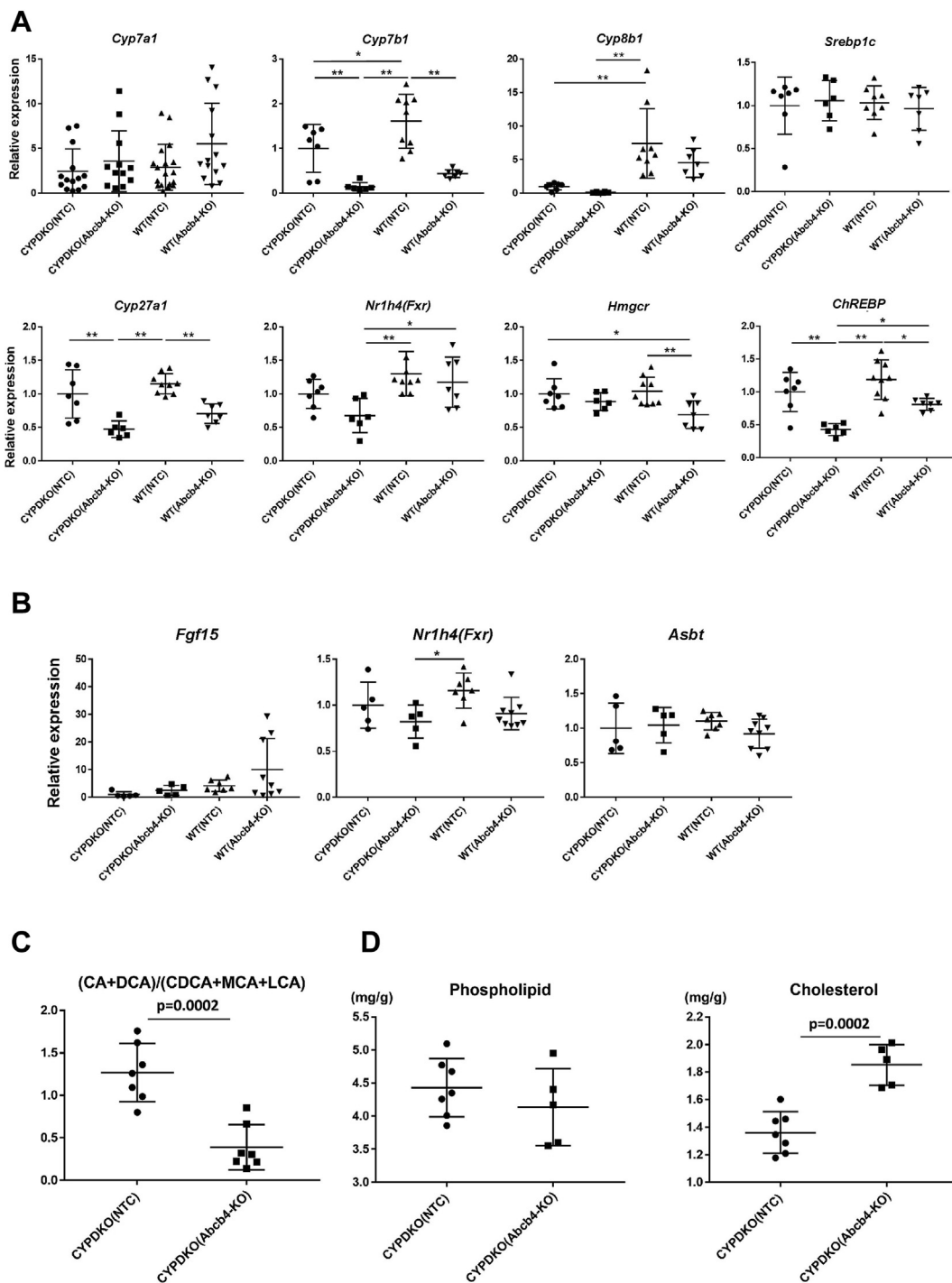


**Fig. 6.** Changes of bile acid metabolic pathways in the Abcb4-deleted CYPDKO mice. A: Expression of bile acid and lipid synthesis-related enzymes and transcription factors in the liver. The expression of genes in CYPDKO/NTC mouse livers was set to 1.0 (n = 7 for CYPDKO/NTC, n = 6 for CYPDKO/Abcb4-KO, n = 9 for WT/NTC, and n = 7 for WT/Abcb4-KO). B: Gene expression changes of bile acid metabolism-related genes in the terminal ileum. The expression of genes in CYPDKO/NTC mouse terminal ileum was set to 1.0 (n = 5 for CYPDKO/NTC, n = 5 for CYPDKO/Abcb4-KO, n = 7 for WT/NTC, and n = 9 for WT/Abcb4-KO). C: (CA + DCA)/(CDCA + MCAs + LCA) ratio of bile acids in the liver derived from the Abcb4-deleted CYPDKO mice (n = 7 for CYPDKO/NTC mouse livers, and n = 7 for CYPDKO/Abcb4-KO mouse livers). D: Phospholipid and cholesterol in the CYPDKO and CYPDKO/Abcb4-KO mouse livers. After extraction of lipids from mice livers, the amount of phospholipid and cholesterol were analyzed (n = 7 for CYPDKO/NTC mouse livers and n = 5 for CYPDKO/Abcb4-KO mouse livers). Results are represented as mean  $\pm$  SD (A, B, One way ANOVA; C, D, Student's *t* test, \**P* < 0.05, \*\**P* < 0.01).

in CYPDKO mouse livers. In contrast, the expression of *Hmgcr*, a cholesterol synthesis enzyme, was downregulated in WT/*Abcb4*-deficient mice. Expression of lipid metabolism-related transcription factors *ChREBP* but not *Srebp1c* was downregulated by *Abcb4*-deletion in both WT and CYPDKO mice. In the small intestine, *Nrlh4* and fibroblast growth factor (FGF) 15 are involved in bile acid metabolism. In mice, expression of *Cyp7a1* is mainly regulated by the intestinal *Fgf15* pathway via *Nrlh4* (29). We analyzed the expression of these genes in the terminal ileum; however, no significant changes were observed in *Fgf15* expression, although a slight decrease of *Nrlh4* expression was observed in CYPDKO/*Abcb4*-deficient mice (Fig. 6B).

As shown above, in wild-type mice livers, more than half of the bile acid composition was of hydrophilic taurine-conjugated MCAs regardless of the presence or absence of *Abcb4* deficiency. In contrast, TDCA was the major bile acid in CYPDKO mice, and TCDCA was the major bile acid in CYPDKO/*Abcb4*-deficient mice (Fig. 5A). In the bile acid metabolic pathways, *Cyp8b1* regulates the ratio of primary bile acid CA and secondary bile acid DCA (CA + DCA) to primary bile acids CDCA,  $\alpha$ MCA, and  $\beta$ MCA and secondary bile acids LCA and  $\omega$ MCA (CDCA + MCAs + LCA). *Cyp27a1* and *Cyp7b1* also regulate the production of (CDCA + MCAs + LCA). Thus, the (CA + DCA)/(CDCA + MCA + LCA) ratio indicates which synthetic pathways and Cyp enzymes are important for bile acid composition. The (CA + DCA)/(CDCA + MCA + LCA) ratio of wild-type mouse livers with or without *Abcb4* deletion was low because of the high concentration of MCA. In contrast, there were very few MCAs in the livers of CYPDKO mice. Therefore, we compared the (CA + DCA)/(CDCA + MCA + LCA) ratio between CYPDKO/NTC and CYPDKO/*Abcb4*-deficient mice. This ratio was significantly decreased by the combination of CYPDKO and *Abcb4*-deletion (Fig. 6C). The synthesis or import of first bile acid CA and second bile acid DCA into the liver might be suppressed by the *Abcb4*-defect.

*Abcb4* is a transporter that supplies phospholipids from hepatocytes to bile, and cholesterol is partially metabolized by bile acids. As shown in Fig. 2, phospholipid and cholesterol levels in the gallbladder bile were significantly downregulated by the deletion of *Abcb4*. We analyzed the hepatic phospholipid and cholesterol levels in CYPDKO/*Abcb4*-deficient mice. Phospholipid levels in the liver remained constant despite *Abcb4* deficiency in CYPDKO mice, suggesting that cell membrane phospholipids, the main components of phospholipids in hepatocytes, are barely altered by the deletion of *Abcb4*. *Abcb4* deletion increased cholesterol levels in the liver (Fig. 6D). The metabolism of cholesterol to bile acids may be inhibited by decreased expression of several CYP genes involved in bile acid synthesis, as observed in CYPDKO/*Abcb4*-deficient mice.

## DISCUSSION

The Cas9 gene and gRNA for the target genes were expressed in vivo using AAVs, making them targets for disease reproducibility and treatment via genome editing (22, 30). In addition, the use of tissue-specific promoters for Cas9 protein expression by AAV enables the rapid induction of tissue-specific gene deletion (25). Here, we used the hAAT promoter as a liver-specific promoter for SaCas9 gene expression. When we analyzed this promoter activity using a genome-editing evaluation system in GFP-mutant mice, it was found to be highly specific, as it did not induce genome-editing in organs other than the liver. The hAAT promoter is very small and suitable while using AAV for the transduction of several genes other than Cas9. A method for introducing gRNA into Cas9-transgenic mice has also been reported as an in vivo gene modification system (16, 31) and these mice were recently used for cholestasis-related gene assays (32). Although this method has the advantage of producing and using less number of AAV, mice strains susceptible to gene modification are limited. Using Cas9-transgenic mice, inducing additional mutations in already established gene-deficient mice is laborious because Cas9-transgenic mice must be mated with target gene-deficient mice. Therefore, developing an enhanced system that efficiently introduces both Cas9 and gRNA in a tissue-specific manner to induce genome editing would be advantageous for analyzing existing gene-knockout mice.

The hydrophobicity of bile acids contributes to the induction of liver injury in cholestasis. Hydrophobic bile acid composition induced by the CA diet in hepatic reductase-null mice is involved in ATP8b1- and *Abcb4*-deletion-induced liver injury (11). In contrast, the addition of hydrophilic tetrahydroxylated bile acid improves cholestatic liver injury in *Abcb4*-knockout mice (28, 33). The major difference in bile acid composition between mice and humans is the high level of hydrophilic MCAs in murine bile, owing to the expression of mouse-specific bile acid-metabolizing enzymes and the abundance of taurine-conjugated bile acids. A human bile acid-like mouse model genetically deleted for the enzyme involved in MCA synthesis was used for these analyses because the toxicity of bile acid is similar to that of human synthesis (12). For example, when CYPDKO mice were treated with UDCA, a therapeutic drug for liver damage, the hydrophobicity of bile acids was reduced, and the liver damage caused by CYPDKO was suppressed in male mice. In contrast, the addition of UDCA increased intrahepatic LCA in female mice, leading to increased liver injury (27). In autoimmune diseases, such as primary biliary cholangitis, human-like changes in bile acid composition caused by CYPDKO affect hepatotoxicity and induce pathological changes (34). Thus, mice with bile acid compositions similar to those of humans are thought to be



extremely useful for analyzing liver damage, such as cholestasis.


In this study, the PFIC3-related gene, *Abcb4*, was analyzed to examine whether human-like bile acid composition alters PFIC physiology in mouse models. We used an AAV-mediated genome-editing system to induce *Abcb4*-deletion in CYPDKO mice. Wild-type mice with an *Abcb4*-deletion have been reported, and increased serum levels of liver injury markers and associated changes in liver tissue (e.g., hyperplasia of bile ducts) have been observed several weeks after birth (28). *Abcb4* is a phospholipid transporter that is transported to the bile. It is possible that *Abcb4* deletion increases bile toxicity by decreasing phospholipid concentrations in bile. We found that phospholipid and cholesterol levels in gallbladder bile were significantly down-regulated by the deletion of *Abcb4* in both wild-type and CYPDKO mice. In addition, total bile acid levels in the serum and liver increased in both WT/*Abcb4*-deficient and CYPDKO/*Abcb4*-deficient mice. However, *Abcb4*-deletion induces more severe liver injury in CYPDKO mice than in wild-type mice. Bile acids in the livers of wild-type mice were predominantly composed of taurine-conjugated CA and taurine-conjugated MCAs. Hydrophobicity indices of total bile acids in the liver revealed a significant difference in hydrophobicity and toxicity between the bile acid compositions of CYPDKO and wild-type mice. *Abcb4* deletion in wild-type mice did not induce severe liver injury after AAV infection in this short-term study (4–5 weeks). In contrast, *Abcb4* deletion induced severe liver injury, bile ductal cell hyperplasia, and fibrosis in CYPDKO mice, which contain more toxic hydrophobic bile acids. These results indicate that the unusual regulation induced by *Abcb4* deletion with humanized hydrophobic bile acid composition may be involved in hepatic injury, apoptosis, and inflammation. As shown in the previous *Abcb4* KO mice reports (9), serum bilirubin was not significantly upregulated. Our study revealed that serum bilirubin levels were not altered by *Abcb4* deletion in the humanized hydrophobic bile acid composition, which induced liver injury and fibrosis. The reason remains unknown but might be due to differences in bilirubin metabolism between humans and mice.

The molecular mechanism by which *Abcb4* deletion induces liver injury remains unclear. Double-knockout mice with *Abcb4* and either the TRAIL receptor or TLR4 revealed that *Abcb4*-deleted liver injury is involved in apoptosis- and inflammation-related mechanisms (35, 36). In addition, several cholesterol and bile acid metabolic pathways were changed by the deletion of *Abcb4*. When *Abcb4* was deleted in CYPDKO mice, the amounts of CDCA, LCA, and UDCA increased in CYPDKO/*Abcb4*-deficient mice, the molecular mechanism underlying the increase in the amount of these bile acids is unknown. Bile acid synthesis is divided into the classic pathway and the

alternative pathways (37). Cyp7a1 and Cyp8b1 mainly regulate the classic pathway and Cyp27a1 and Cyp7b1 mainly regulate the alternative pathway. Particularly, Cyp8b1 determines the balance of CA and CDCA through the classic pathway. In this study, CYP8b1 was significantly suppressed in both CYPDKO/NTC- and CYPDKO/*Abcb4*-deficient mice, suggesting that a different mechanism is responsible for the alteration of bile acid composition in *Abcb4* deficiency. In addition, secondary bile acids, such as DCA, LCA, and UDCA, are metabolized in the intestine. These metabolic interactions in both the liver and intestine may have caused the formation of a specific bile acid composition and contributed to severe liver injury in CYPDKO/*Abcb4*-deficient mice.

In a conventional PFIC3 mouse model, the *abcb4* gene deletion was induced in wild-type mice, which have a high content of hydrophilic bile acids, resulting in a longer time required for the induction of liver damage and fibrosis. In this study, using CYPDKO mice with a human-like bile acid composition, we established a PFIC3 mouse model that more closely resembles the human pathology. In addition to PFIC, bile acid-related diseases, including primary biliary cholangitis, may be affected by differences in bile acid composition in analyses using a mouse model. Methods for introducing new mutations into existing CYPDKO mice include genome-editing of fertilized eggs from CYPDKO mice or mating existing *Abcb4*-deficient and CYPDKO mice. However, these methods require a considerable amount of time to establish the desired mouse strain. Using a method in which SaCas9 and target gRNAs were introduced using AAV to induce gene deletion via genome-editing in vivo, we detected phenotypic differences in *Abcb4* deletions between wild-type and CYPDKO mice. The combination of human bile acid-like CYPDKO mice and the rapid genome-editing method using AAV demonstrated in this study may be useful for the rapid analysis of various bile acid-related diseases in mouse models. In addition, elucidation and development of treatment methods are expected to be the result of studies using mouse models.

#### Data availability

Data are available from the corresponding author upon reasonable request. 

#### Supplemental data

This article contains [supplemental data](#).

#### Acknowledgment

*Assistance with the study:* Some analyses were performed by the Medical Science College Office of Tokai University.

#### Author contributions

K. I., T. A., K. Y., Y. M., A. H., S. I., A. K., and K. T. investigation; K. Y., A. K., and K. T. writing—original draft; Y. I., A. H., M. O., and T. K. writing—review & editing; Y. I., T. K., and

A. K. conceptualization. A. H., M. O. resources; A. H., A. K. methodology.

#### Author ORCIDs

Kota Tsuruya  <https://orcid.org/0000-0002-9884-8039>

Yutaka Inagaki  <https://orcid.org/0000-0001-6640-7688>

Akira Honda  <https://orcid.org/0000-0003-0902-8272>

#### Funding and additional information

This study was supported in part by a Grant-in-Aid for Scientific Research (MEXT KAKENHI Grant Number JP20H04931 and JSPS KAKENHI Grant Number JP19H03643 to A. K. and JP22K08062 to T. K.). This study was supported in part by the Tokai University School of Medicine Research Aid and the 2022–2023 Tokai University School of Medicine Project Research.

#### Conflicts of interest

The authors declare that they have no known competing financial interests or personal relationships that could have appeared to influence the work reported in this paper:

The author, Akira Honda, is an Editorial Board Member for *Journal of Lipid Research* and was not involved in the editorial review or the decision to publish this article.

#### Abbreviations

AAV, adeno-associated virus; ALT, alanine aminotransferase; AST, aspartate aminotransferase; CA, cholic acid; CDCA, chenodeoxycholic acid; CYPDKO, Cyp2c70Cyp2a12 double-deficient mice; GFP, green fluorescent protein; hAAT, human antitrypsin; HI, Hydrophobicity index; LCA, lithocholic acid; MCAs, muricholic acid; PFIC, progressive familial intrahepatic cholestasis; gRNA, guide RNA; UDCA, ursodeoxycholic acid.

Manuscript received September 30, 2023, and in revised form July 29, 2024. Published, JLR Papers in Press, August 5, 2024, <https://doi.org/10.1016/j.jlr.2024.100616>

## REFERENCES

1. Sinal, C. J., Tohkin, M., Miyata, M., Ward, J. M., Lambert, G., and Gonzalez, F. J. (2000) Targeted disruption of the nuclear receptor FXR/BAR impairs bile acid and lipid homeostasis. *Cell* **102**, 731–744
2. Cariello, M., Piccinin, E., Garcia-Irigoyen, O., Sabba, C., and Moschetta, A. (2018) Nuclear receptor FXR, bile acids and liver damage: introducing the progressive familial intrahepatic cholestasis with FXR mutations. *Biochim. Biophys. Acta Mol. Basis Dis.* **1864**, 1308–1318
3. Pfister, E. D., Droge, C., Liebe, R., Stalke, A., Buhl, N., Ballauff, A., et al. (2022) Extrahepatic manifestations of progressive familial intrahepatic cholestasis syndromes: presentation of a case series and literature review. *Liver Int.* **42**, 1084–1096
4. Bull, L. N., and Thompson, R. J. (2018) Progressive familial intrahepatic cholestasis. *Clin. Liver Dis.* **22**, 657–669
5. Buschman, E., Arcenci, R. J., Croop, J. M., Che, M., Arias, I. M., Housman, D. E., et al. (1992) mdr2 encodes P-glycoprotein expressed in the bile canalicular membrane as determined by isoform-specific antibodies. *J. Biol. Chem.* **267**, 18093–18099
6. Oude Elferink, R. P., Ottenhoff, R., van Wijland, M., Smit, J. J., Schinkel, A. H., and Groen, A. K. (1995) Regulation of biliary lipid secretion by mdr2 P-glycoprotein in the mouse. *J. Clin. Invest.* **95**, 31–38
7. Oude Elferink, R. P., Ottenhoff, R., van Wijland, M., Frijters, C. M., van Nieuwkerk, C., and Groen, A. K. (1996) Uncoupling of biliary phospholipid and cholesterol secretion in mice with reduced expression of mdr2 P-glycoprotein. *J. Lipid Res.* **37**, 1065–1075
8. Fickert, P., Fuchsbichler, A., Wagner, M., Zollner, G., Kaser, A., Tilg, H., et al. (2004) Regurgitation of bile acids from leaky bile ducts causes sclerosing cholangitis in Mdr2 (Abcb4) knockout mice. *Gastroenterology* **127**, 261–274
9. Lammert, F., Wang, D. Q., Hillebrandt, S., Geier, A., Fickert, P., Trauner, M., et al. (2004) Spontaneous cholecysto- and hepatolithiasis in Mdr2<sup>-/-</sup> mice: a model for low phospholipid-associated cholelithiasis. *Hepatology* **39**, 117–128
10. Ikenaga, N., Liu, S. B., Sverdlow, D. Y., Yoshida, S., Nasser, I., Ke, Q., et al. (2015) A new Mdr2<sup>(-/-)</sup> mouse model of sclerosing cholangitis with rapid fibrosis progression, early-onset portal hypertension, and liver cancer. *Am. J. Pathol.* **185**, 325–334
11. Kunne, C., de Graaff, M., Duijst, S., de Waart, D. R., Oude Elferink, R. P., and Paulusma, C. C. (2014) Hepatic cytochrome P450 deficiency in mouse models for intrahepatic cholestasis predispose to bile salt-induced cholestasis. *Lab. Invest.* **94**, 1103–1113
12. Honda, A., Miyazaki, T., Iwamoto, J., Hirayama, T., Morishita, Y., Monma, T., et al. (2020) Regulation of bile acid metabolism in mouse models with hydrophobic bile acid composition. *J. Lipid Res.* **61**, 54–69
13. Yin, H., Xue, W., Chen, S., Bogorad, R. L., Benedetti, E., Grompe, M., et al. (2014) Genome editing with Cas9 in adult mice corrects a disease mutation and phenotype. *Nat. Biotechnol.* **32**, 551–553
14. Jinek, M., Chylinski, K., Fonfara, I., Hauer, M., Doudna, J. A., and Charpentier, E. (2012) A programmable dual-RNA-guided DNA endonuclease in adaptive bacterial immunity. *Science* **337**, 816–821
15. Cong, L., Ran, F. A., Cox, D., Lin, S., Barretto, R., Habib, N., et al. (2013) Multiplex genome engineering using CRISPR/Cas systems. *Science* **339**, 819–823
16. Platt, R. J., Chen, S., Zhou, Y., Yim, M. J., Swiech, L., Kempton, H. R., et al. (2014) CRISPR-Cas9 knockin mice for genome editing and cancer modeling. *Cell* **159**, 440–455
17. Swiech, L., Heidenreich, M., Banerjee, A., Habib, N., Li, Y., Trombetta, J., et al. (2015) In vivo interrogation of gene function in the mammalian brain using CRISPR-Cas9. *Nat. Biotechnol.* **33**, 102–106
18. Ran, F. A., Cong, L., Yan, W. X., Scott, D. A., Gootenberg, J. S., Kriz, A. J., et al. (2015) In vivo genome editing using Staphylococcus aureus Cas9. *Nature* **520**, 186–191
19. Cunningham, S. C., Dane, A. P., Spinoulas, A., and Alexander, I. E. (2008) Gene delivery to the juvenile mouse liver using AAV2/8 vectors. *Mol. Ther.* **16**, 1081–1088
20. Wang, L., Wang, H., Bell, P., McCarter, R. J., He, J., Calcedo, R., et al. (2010) Systematic evaluation of AAV vectors for liver directed gene transfer in murine models. *Mol. Ther.* **18**, 118–125
21. Thakore, P. I., Kwon, J. B., Nelson, C. E., Rouse, D. C., Gemberling, M. P., Oliver, M. L., et al. (2018) RNA-guided transcriptional silencing in vivo with S. aureus CRISPR-Cas9 repressors. *Nat. Commun.* **9**, 1674
22. Yang, Y., Wang, L., Bell, P., McMenamin, D., He, Z., White, J., et al. (2016) A dual AAV system enables the Cas9-mediated correction of a metabolic liver disease in newborn mice. *Nat. Biotechnol.* **34**, 334–338
23. He, X., Zhang, Z., Xue, J., Wang, Y., Zhang, S., Wei, J., et al. (2022) Low-dose AAV-CRISPR-mediated liver-specific knock-in restored hemostasis in neonatal hemophilia B mice with subtle antibody response. *Nat. Commun.* **13**, 7275
24. Liu, Z., Chen, S., Xie, W., Song, Y., Li, J., Lai, L., et al. (2022) Versatile and efficient in vivo genome editing with compact Streptococcus pasteurianus Cas9. *Mol. Ther.* **30**, 256–267
25. Ohmori, T., Nagao, Y., Mizukami, H., Sakata, A., Muramatsu, S. I., Ozawa, K., et al. (2017) CRISPR/Cas9-mediated genome editing via postnatal administration of AAV vector cures haemophilia B mice. *Sci. Rep.* **7**, 4159
26. Miura, H., Imafuku, J., Kurosaki, A., Sato, M., Ma, Y., Zhang, G., et al. (2021) Novel reporter mouse models useful for evaluating in vivo gene editing and for optimization of methods of delivering genome editing tools. *Mol. Ther. Nucleic Acids* **24**, 325–336
27. Ueda, H., Honda, A., Miyazaki, T., Morishita, Y., Hirayama, T., Iwamoto, J., et al. (2022) Sex-, age-, and organ-dependent improvement of bile acid hydrophobicity by ursodeoxycholic acid treatment: a study using a mouse model with human-like bile acid composition. *PLoS One* **17**, e0271308

28. Wang, R., Sheps, J. A., Liu, L., Han, J., Chen, P. S. K., Lamontagne, J., *et al.* (2019) Hydrophilic bile acids prevent liver damage caused by lack of biliary phospholipid in Mdr2(-/-) mice. *J. Lipid Res.* **60**, 85–97
29. Kong, B., Wang, L., Chiang, J. Y., Zhang, Y., Klaassen, C. D., and Guo, G. L. (2012) Mechanism of tissue-specific farnesoid X receptor in suppressing the expression of genes in bile-acid synthesis in mice. *Hepatology*. **56**, 1034–1043
30. De Giorgi, M., Li, A., Hurley, A., Barzi, M., Doerfler, A. M., Cherayil, N. A., *et al.* (2021) Targeting the Apoal locus for liver-directed gene therapy. *Mol. Ther. Methods Clin. Dev.* **21**, 656–669
31. Jarrett, K. E., Lee, C. M., Yeh, Y. H., Hsu, R. H., Gupta, R., Zhang, M., *et al.* (2017) Somatic genome editing with CRISPR/Cas9 generates and corrects a metabolic disease. *Sci. Rep.* **7**, 44624
32. Wakasa, K., Tamura, R., Osaka, S., Takei, H., Asai, A., Nittono, H., *et al.* (2024) Rapid in vivo evaluation system for cholestasis-related genes in mice with humanized bile acid profiles. *Hepatology. Commun.* **8**, e0382
33. Fuchs, C. D., Dixon, E. D., Hendriks, T., Mlitz, V., Wahlstrom, A., Stahlman, M., *et al.* (2022) Tetrahydroxylated bile acids improve cholestatic liver and bile duct injury in the Mdr2(-/-) mouse model of sclerosing cholangitis via immunomodulatory effects. *Hepatology. Commun.* **6**, 2368–2378
34. Yamashita, M., Honda, A., Shimoyama, S., Umemura, M., Ohta, K., Chida, T., *et al.* (2023) Breach of tolerance versus burden of bile acids: resolving the conundrum in the immunopathogenesis and natural history of primary biliary cholangitis. *J. Autoimmun.* **136**, 103027
35. Weber, S. N., Bohner, A., Dapito, D. H., Schwabe, R. F., and Lammert, F. (2016) TLR4 deficiency protects against hepatic fibrosis and diethylnitrosamine-induced pre-carcinogenic liver injury in fibrotic liver. *PLoS One* **11**, e0158819
36. Krishnan, A., Katsumi, T., Guicciardi, M. E., Azad, A. I., Ozturk, N. B., Trussoni, C. E., *et al.* (2020) Tumor necrosis factor-related apoptosis-inducing ligand receptor deficiency promotes the ductular reaction, macrophage accumulation, and hepatic fibrosis in the Abcb4(-/-) mouse. *Am. J. Pathol.* **190**, 1284–1297
37. Russell, D. W. (2003) The enzymes, regulation, and genetics of bile acid synthesis. *Annu. Rev. Biochem.* **72**, 137–174